

Friedel oscillations in a two-band Hubbard model for CuO chains

著者	前川 禎通
journal or publication title	Physical review. B
volume	69
number	1
page range	014513-1-014513-7
year	2004
URL	http://hdl.handle.net/10097/40315

doi: 10.1103/PhysRevB.69.014513

Friedel oscillations in a two-band Hubbard model for CuO chainsM. Mori,¹ T. Tohyama,¹ S. Maekawa,¹ and J. A. Riera^{1,2,3}¹*Institute for Materials Research, Tohoku University, Sendai 980-8577, Japan*²*Instituto de Física Rosario, Consejo Nacional de Investigaciones Científicas y Técnicas, y Departamento de Física, Universidad Nacional de Rosario, Avenida Pellegrini 250, 2000-Rosario, Argentina*³*Laboratoire de Physique Théorique CNRS-FRE2603, Université Paul Sabatier, F-31062 Toulouse, France*

(Received 30 August 2003; published 28 January 2004)

Friedel oscillations induced by open boundary conditions in a two-band Hubbard model for CuO chains are numerically studied. We find that for physically realistic parameters and close to quarter filling, these oscillations have a $2k_F$ modulation according with experimental results on $\text{YBa}_2\text{Cu}_3\text{O}_{7-\delta}$. In addition, we predict that, for the same parameters, as hole doping is reduced from quarter filling to half filling, Friedel oscillations would acquire a $4k_F$ modulation, typical of a strongly correlated electron regime. The $4k_F$ modulation also dominates in the electron doped region. The range of parameters varied is very broad, and hence the results reported could apply to other cuprates and other strongly correlated compounds with quasi-one-dimensional structures. On a more theoretical side, we stress the fact that the copper and oxygen subsystems should be described by two different Luttinger liquid exponents.

DOI: 10.1103/PhysRevB.69.014513

PACS number(s): 71.10.Fd, 71.10.Hf, 71.10.Pm

I. INTRODUCTION

The application of scanning tunneling spectroscopy (STM) techniques to the CuO chain planes in $\text{YBa}_2\text{Cu}_3\text{O}_{7-\delta}$ (YBCO) has provided insights into the physics of these quasi-one dimensional (1D) electronic structures. These experimental studies have shown, in real space, the presence of charge modulations along the chains at low temperature, inside the superconducting phase.^{1,2} These charge oscillations had been inferred earlier from neutron scattering experiments on the same compound.³ Taking together results from both band calculations⁴ and angle-resolved photoemission⁵ (ARPES) indicating a chain filling close to one quarter, it turns out that the observed charge modulations have a $2k_F$ wave number.

Although earlier STM studies⁶ gave indications of the presence of charge oscillations on the chains, the present interest in these features comes from a more recent set of experiments exploring the interplay between the chain plane and the CuO_2 plane in YBCO. On the one hand, the chains (running along the **b** direction) may contribute to the in-plane resistivity anisotropy in this compound.⁷ It is also important to notice that stripes in CuO_2 planes also run along the **b** direction, maybe not coincidentally. On the other hand, there have been experimental indications of a superfluid density induced on the chains due to the proximity to the CuO_2 planes.^{8,9} Although the interpretation of this last set of experiments is still controversial,^{5,10} one recent theoretical study¹¹ offers an explanation of STM results¹ based on this scenario of proximity induced chain superconductivity (SC). In this model, the resonances in the chains arise from the interference between magnetic impurities in the chains.

Alternatively, we believe it is necessary to search for explanations of these experimental results based on models which capture the intrinsic electronic interactions on the chains. Eventually, in this kind of model, the SC on the CuO_2 planes could modify at an effective level the coupling constants of the intrachain interactions. This approach con-

nects the present study to the more general theoretical interest in various types of charge inhomogeneities appearing in strongly correlated electron systems in low spatial dimensions. In fact, in addition to the relevance of the presence of charge oscillations in the chains to the physics of the CuO_2 planes, it has been emphasized that precisely the assumed strong Coulomb interactions in the cuprates would naively favor a $4k_F$ wave number instead of the observed $2k_F$ wave number of the charge modulations.²

Since CuO chains are cut by oxygen depletion, we will try to describe the charge modulations as generalized Friedel oscillations (FO's) starting at the open end of the resulting fragments. A very recent numerical and analytical study¹² on the 1D one-band Hubbard model indeed found a crossover from $2k_F$ to $4k_F$ FO's as the strength of the on-site Coulomb interaction U is increased. We are going to examine a two-band Hubbard model, appropriate for CuO chains,¹³ where the situation is more complex due to different Coulomb repulsions on Cu and O ions, in addition to the charge transfer between them.¹⁴ It is interesting to notice that ARPES shows⁵ a chain's Fermi surface in agreement with band calculations, and at the same time the dispersion along the chain direction agrees with the holon band predicted by strongly correlated theories.¹⁵ Hence, although the Coulomb repulsion on Cu ions is large, it does not automatically imply a strongly correlated behavior on any given physical quantity. In particular, we will show a complex dependence of $2k_F$ and $4k_F$ FO's with respect to the Coulomb interactions and charge transfer parameter.

The model here studied does not include electron-lattice coupling, which is another possibility of inducing $2k_F$ instabilities. Experimentally,³ it has been suggested that standard lattice phonons are unlikely to reproduce the observed features. Finally, both in order to help the understanding of our results and in order to extend the scope of this study, we will consider a somewhat large variation of interaction parameters, and, in addition to quarter filling, dopings close to half filling, and also electron doped chains will also be studied. In

addition, we will consider open ends occupied with O ions and Cu ions.

This paper is structured as follows. In Sec. II, we describe the model and method of calculation, and we show the numerical results for density oscillations. The theoretical and experimental implications of these results are discussed in Sec. III.

II. $2k_F/4k_F$ PHASE BOUNDARY

A. Model and method of calculation

The model studied is the 1D two-band Hubbard model defined as

$$\begin{aligned} \mathcal{H} = & -t_{pd} \sum_{i,\sigma} (c_{2i-1\sigma}^\dagger c_{2i\sigma} + \text{H.c.}) + U_d \sum_i n_{2i-1\uparrow} n_{2i-1\downarrow} \\ & + U_p \sum_i n_{2i\uparrow} n_{2i\downarrow} + U_{pd} \sum_i n_{2i-1} n_{2i} + \Delta \sum_i n_{2i}, \quad (1) \end{aligned}$$

where, $c_{j\sigma}^\dagger$ creates a hole with spin σ at site j , $n_{j\sigma} = c_{j\sigma}^\dagger c_{j\sigma}$, $n_j = n_{j\uparrow} + n_{j\downarrow}$. The sums run over $i=1, \dots, L$ (L is the number of unit cells), and Cu (O) ions occupy odd (even) sites. $t_{pd}=1$. All our results shown below correspond to $U_d=8$, $U_{pd}=0$, and $U_p, \Delta < U_d$. The number of holes (N_h) is larger than L for hole doped systems in which case the filling is computed as $n_h = (2L - N_h)/L$, or smaller than L for electron doped systems in which case the filling is computed as $n_e = N_h/L$. At half filling $n_h = n_e = 1$. The numerical technique employed in the present study is the density matrix renormalization group algorithm (DMRG).¹⁶ The most important quantity measured by this technique is the on-site charge density, $n(i) = \langle n_i \rangle$. Most results were obtained with a truncation number $m=200$. For several cases we also examined $m=300$ and 400 with almost indistinguishable results.

In principle, we are interested in the effect of oxygen depletion which implies that CuO chains are cut at oxygen sites. These depleted oxygens could be modeled by just imposing open boundary conditions on chains with odd numbers of sites with the two end sites corresponding to Cu ions. However, it is technically convenient to use chains with even numbers of sites which implies that one end is occupied by an oxygen ion and the other end site by a copper ion. The open end with an O ion would correspond to a nonmagnetic impurity, for example a Zn ion replacing a Cu ion.¹⁷ If one assumes that Friedel oscillations from both ends do not have nonlinear superpositions, i.e., both oscillations are independent of each other, then the use of even numbers of sites allows us to simultaneous study both types of impurities in a single chain.

Since, as stated in Sec. I, Friedel oscillations appear due to oxygen depleted sites acting as impurity centers in an otherwise metallic chain, then they will follow a power law behavior predicted by Luttinger liquid theory,¹⁸

$$n(r) - n_0 \sim a_1 \frac{\cos(2k_F r + \phi_1)}{r^{(1+K_\rho)/2}} + a_2 \frac{\cos(4k_F r + \phi_2)}{r^{2K_\rho}}, \quad (2)$$

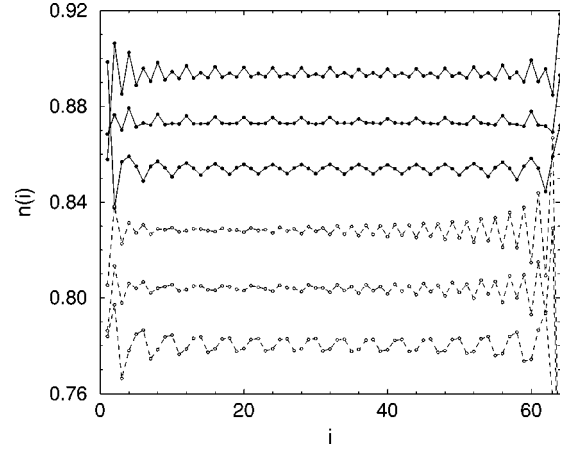


FIG. 1. Density at site i for $L=64$, $n_h=0.5$, $U_d=8$, $U_p=2$, $U_{pd}=0$, and $\Delta=2, 4$, and 5 from bottom to top. O sites: open symbols; Cu sites: filled symbols. The curves have been arbitrarily shifted for the sake of clarity.

with r the distance from the impurity. This expression can be derived from the asymptotic form of the charge correlations (neglecting logarithmic corrections to the $2k_F$ term) and K_ρ is the interaction dependent correlation exponent.¹⁹ Numerical studies have verified that FO's follow this form for the one-band Hubbard and t - J models on chains and ladders^{12,20} and for the Kondo lattice model on chains.²¹ In the following, we will fit our data using Eq. (2). The inclusion of finite size corrections^{19,22} to Eq. (2) would in principle lead to a better fitting of the numerical results. However, as discussed in Ref. 20, the finite size dependence is considerably reduced by disregarding the first few sites close to the ends of the chain. In addition, we believe that for the chain length here considered ($L=64$) finite size corrections would fall within the error bars in Figs. 3 and 6. The complete fitting procedure is detailed in the Appendix. The key point of this procedure is that we *simultaneously* fit the FO's starting from the left chain end (Cu site) and the one which starts from the right chain end (O site).

B. Quarter filling

We start by examining the electron density $n(i)$ as a function of the position obtained by the DMRG for $L=64$, $N_h=96$, which corresponds to quarter filling, $n_h=0.5$, as a function of U_p and Δ . At this filling, the density modulation has period of four unit cell spacings for the $2k_F$ component. This period can be clearly seen in the Friedel oscillations shown in Fig. 1 ($U_p=2$) in both Cu and O ions, at $\Delta=2$. These density oscillations extend appreciably over the whole chain. For $\Delta=5$, the density oscillations on both types of ions present a period of 2 which corresponds to a $4k_F$ wave. Also shown are the oscillations for $\Delta=4$, close to the cross-over between both regimes.

By applying the fitting procedure previously discussed, we are able to obtain the mean amplitudes for the $2k_F$ and $4k_F$ components of the Friedel oscillations on Cu or on O ions starting at site 1 (occupied by a Cu ion), corresponding to an impurity on an O ion, and the one starting at site 64

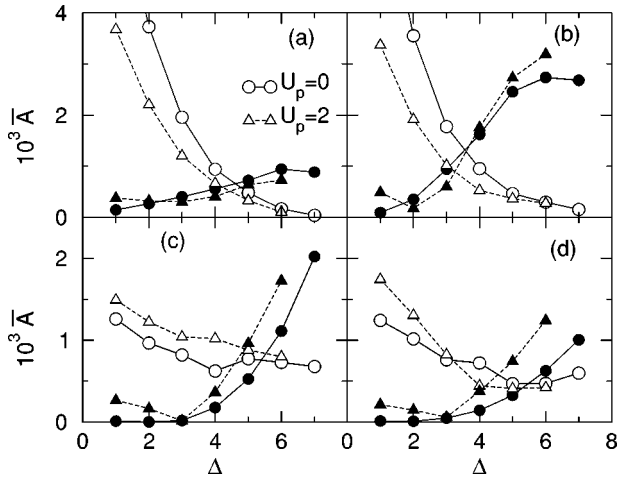


FIG. 2. Δ dependence of the mean amplitude of $2k_F$ (open symbols) and $4k_F$ (filled symbols) components for $U_d=8$, $L=64$, and various values of U_p at $n_h=0.5$. (a) O density oscillations, O impurity. (b) O density oscillations, Cu impurity. (c) Cu density oscillations, O impurity. (d) Cu density oscillations, Cu impurity.

(occupied by an O ion), corresponding to an impurity on a Cu ion. These mean amplitudes are defined by Eqs. (A4) and (A5). The inclusion of the density oscillation close to the ends introduces somewhat large numerical errors, so we discarded the first three points near the ends. The results are depicted in Fig. 2. The error bars are about the size of the symbols used. By discarding different numbers of initial sites of course the amplitudes vary. However, their crossing point does not change appreciably. Various features can be rapidly appreciated: a larger amplitude on O sites than on Cu sites for the dominant component, the suppression of the $2k_F$ amplitude with increasing U_p for O-site oscillations, and larger (smaller) O (Cu) amplitudes for Cu-impurity than for O-impurity.

The crossing of these mean amplitudes as Δ is increased for a given value of U_p is adopted as the crossing of the $2k_F$ -dominated regime to the $4k_F$ -dominated regime. Other criteria could be eventually adopted but we found that this criterion faithfully reproduces the change of oscillation period which is the quantity measured in STM experiments. The results can be summarized in the “phase” diagram shown in Fig. 3. The region of Δ below the crossover corresponds to the $2k_F$ -dominated regime while the region of Δ above it corresponds to the $4k_F$ -dominated regime. The first remarkable feature is that the crossover in the O-ion oscillations takes place at lower values of Δ than the crossover in the Cu-ion oscillations.

To help the interpretation of these results, we have overimposed on this figure lines of constant J/t_{eff} of an effective one-band t - J model, with²³

$$J = \frac{4t_{pd}^4}{\Delta^2} \left(\frac{1}{U_d} + \frac{2}{2\Delta + U_p} \right) \quad (3)$$

and

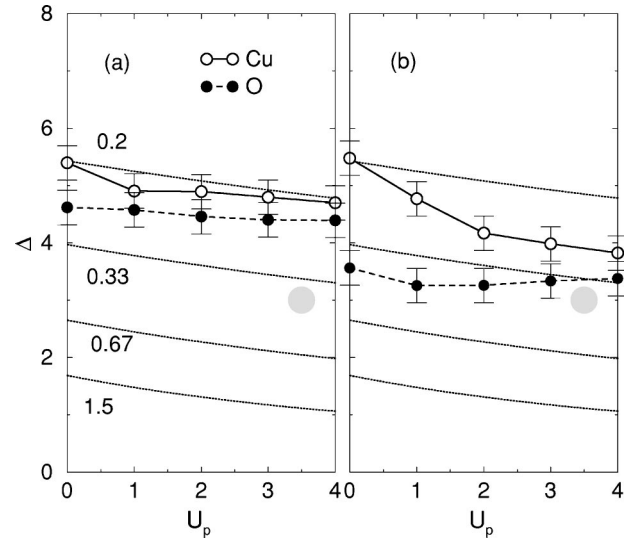


FIG. 3. Phase boundary between the $2k_F$ and $4k_F$ Friedel oscillations at quarter filling for $U_d=8$ and $L=64$. (a) O impurity. (b) Cu impurity. Open circles: boundary of Cu oscillations; filled circles: boundary for O oscillations. Dotted lines are lines of constant J/t_{eff} of the effective one band t - J model (see the text). The gray circles correspond approximately to the physical region of CuO chains.

$$t_{eff} \sim \frac{t_{pd}^2}{\Delta}. \quad (4)$$

We have fixed the proportionality constant in such a way that the physical point for the CuO chains corresponds to $J/t_{eff} = 0.35-0.4$, taking into account some dispersion on the values reported for the Coulomb interactions which are approximately, $U_d \sim 8$ (the value adopted in the present study), $U_p \sim 3-4$ and $\Delta \sim 3$ (in units of t_{pd}). At a fixed hole density, each line of constant J/t_{eff} (indicated in Fig. 3) corresponds in the effective 1D t - J model to a line of constant K_ρ , which have been previously estimated.²⁵ Then, it can be appreciated in Fig. 3 that the $2k_F/4k_F$ boundaries are roughly parallel to these lines with the largest deviation corresponding to the O oscillations and the Cu impurity. In addition, as it can be seen in Fig. 3(a), for the physical region corresponding to the CuO chains (indicated with a gray circle), the FO’s generated by oxygen depletion have $2k_F$ modulation in agreement with experimental results near quarter filling.² In the case of Cu impurity [Fig. 3(b)], although the $2k_F/4k_F$ boundary is shifted to lower values of Δ , the FO’s are predicted to have also a $2k_F$ character in the physical region.

C. $n_h=0.875$ filling

While in the undoped compound, $\text{YBa}_2\text{Cu}_3\text{O}_7$, the chain filling is $n_h=0.5$, upon oxygen depletion it increases toward half-filling, which is reached at $\delta \approx 0.36$ (Ref. 24). Hence, in this subsection we consider the case of $n_h=0.875$. Although increased O depletion would produce, on average, shorter CuO segments, in order to reduce the number of varying parameters and to facilitate the comparison, we study the

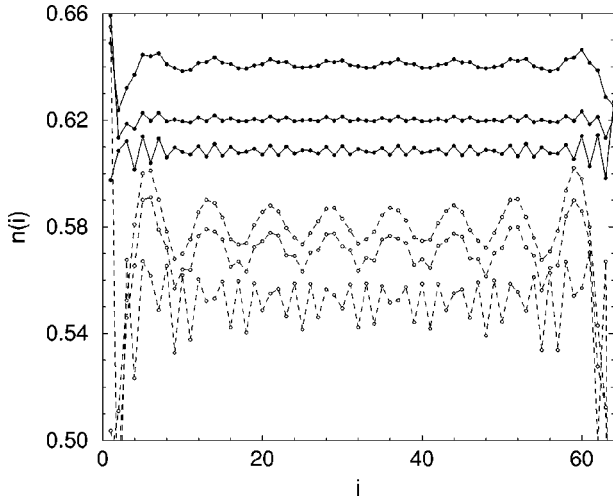


FIG. 4. Density at site i for $L=64$, $n_h=0.875$, $U_d=8$, $U_p=0$, $U_{pd}=0$, and $\Delta=1, 3$, and 5 from bottom to top. O sites: open symbols; Cu sites: filled symbols. The curves have been arbitrarily shifted for the sake of clarity.

same chain length as in Sec. II B, i.e., $L=64$. The filling $n_h=0.875$ then corresponds to $N_h=72$ holes. In this case, $2k_F=7\pi/8$ and $4k_F=\pi/4$.

Let us start by examining in real space density oscillations corresponding to this filling. They are illustrated in Fig. 4. The oscillations for small Δ , corresponding to $2k_F$, can be regarded as period 2 oscillations with kinks, while the oscillations at large Δ , corresponding to $4k_F$ have a well defined period 8 unit cell spacings.

As we did in Sec. II B, we have fitted the density oscillations for both Cu and O ions, and the results for the mean amplitudes of the $2k_F$ and $4k_F$ components are shown in Fig. 5. By comparing with the previous results at quarter filling, it can be concluded that the amplitudes of the dominant component are in general much larger in this case of $n_h=0.875$. Again O oscillations, in general, have larger amplitudes than the Cu ones. It can be also observed that the effect of U_p is relatively small in the present case. Also there are virtually no differences between the cases of O and Cu impurities.

Again, the crossing points between $2k_F$ and $4k_F$ components of the mean amplitudes lead to the “phase” diagram shown in Fig. 6. As anticipated by the previous figure, the boundary between the $2k_F$ (low Δ) and the $4k_F$ (high Δ) regions has been considerably shifted to lower values of Δ with respect to the quarter filled case. As for $n_h=0.5$, these boundaries also approximately follow the lines of constant K_ρ of the effective 1D t - J model. However, in contrast with that case, there is much less difference between the boundaries for O depletion-induced FO’s [Fig. 6(a)] and the boundaries for the FO’s induced by nonmagnetic substitution of Cu ions [Fig. 6(b)]. In any case, as in the quarter filled case, the most remarkable feature is again that the $2k_F$ to $4k_F$ crossover for oxygen FO’s takes place at smaller values of Δ than the one for Cu FO. Notice that for this filling the physical region of parameters (gray circles) falls now on the $4k_F$ side of the diagram.

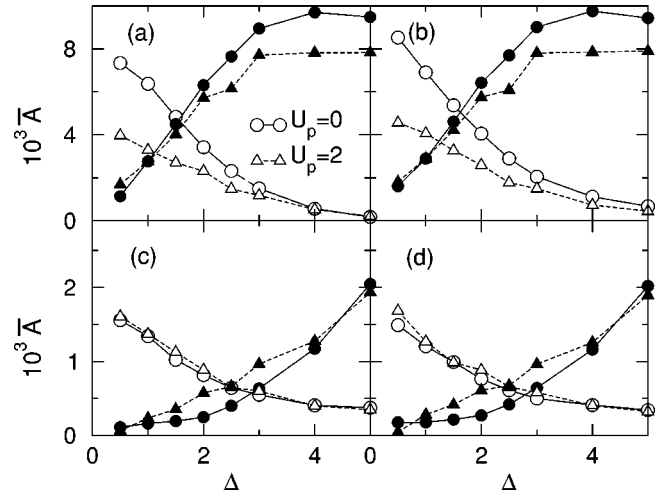


FIG. 5. Same as Fig. 2 but for $n_h=0.875$.

Finally, by further oxygen depletion, $\delta>0.36$, the chain would formally go into the electron doped region. The $2k_F/4k_F$ boundary between Friedel oscillations on Cu ions in the electron doped, $n_e=0.875$, system is also included in Fig. 6. This result confirms the trend suggested by the cases $n_h=0.5$ and $n_h=0.875$, that by reducing the number of holes this boundary shifts to lower values of Δ for a fixed U_p . On the other hand, the occupancy on O sites is very low and we observed $2k_F$ oscillations for all values of the parameters examined. It is reasonable to speculate that by further reducing the number of holes the presence of $4k_F$ oscillations on Cu ions will eventually disappear as well, i.e., the effects of strong electron correlations are expected to be more important close to half filling.

D. Global properties

Let us examine some global properties like the total ground state energy E_0 and the average amplitude of FO. Since this energy is monotonically increasing with Δ , with all the other parameters fixed, it is more meaningful to analyze the quantity obtained by subtracting from E_0 the quantity Δn_O , where n_O is the average filling on O sites. The average of the amplitude of the FO on Cu sites is defined as

$$A_{Cu} = \frac{1}{L} \sum_i |n(i) - n_{Cu}|, \quad (5)$$

where the sum runs over Cu sites and n_{Cu} is the average filling on Cu sites. To be consistent with the fitting procedure and hence to allow a comparison with Figs. 2 and 5, we discarded the first three sites close to both chain ends. The resulting quantity is shown in Figs. 7(a) and 7(b) for $n_h=0.5$ and 0.875 , respectively. It can be noticed that it presents a minimum at a value of Δ close to the $2k_F/4k_F$ boundary of Cu FO at a given value of U_p . As it can be seen in Figs. 7(c) and 7(d), the corrected energy, $E_0 - \Delta n_O$ also presents a minimum at approximately the same values of Δ for $n_h=0.5$. At $n_h=0.875$, the minimum of this quantity is located at a lower value, closer to the $2k_F/4k_F$ boundary of oxygen FO’s.

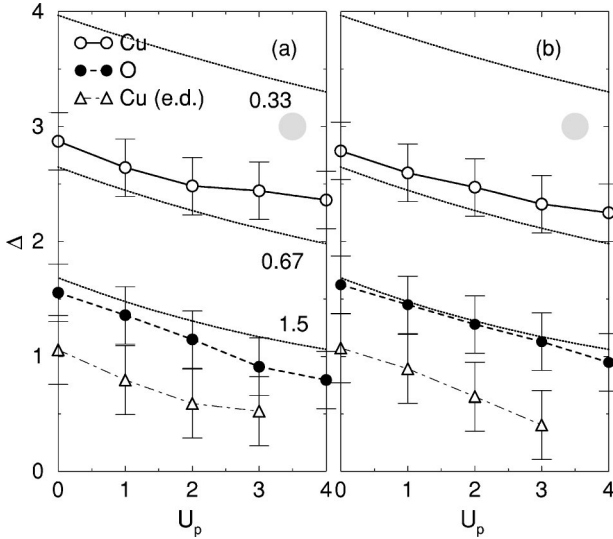


FIG. 6. Phase boundary between the $2k_F$ and $4k_F$ Friedel oscillations for $U_d=8$, $L=64$, $n_h=0.875$. (a) O impurity. (b) Cu impurity. Open circles: boundary of Cu oscillations; filled circles: boundary for O oscillations. Open triangles correspond to Cu oscillations in electron doped, $n_e=0.875$, chains. The gray circles correspond approximately to the physical region of CuO chains.

III. DISCUSSIONS AND CONCLUSIONS

The two most important results of the present study, which can be deduced from Figs. 3 and 6 are (i) the $2k_F$ to $4k_F$ crossover takes place at smaller values of Δ for given U_p as doping is reduced from quarter filling to half filling; and (ii) for hole doped chains this crossover takes place at smaller Δ for the density oscillations on O ions than for the ones on Cu ions. Let us discuss these two features in detail.

In the first place, the fact that the $2k_F/4k_F$ boundaries quite likely correspond to lines of constant K_ρ of an effective 1D t - J model suggests that both the approximate mapping of this model and the whole fitting procedure are physically correct. One should notice that this effective one-band model is obtained essentially by projecting out the oxygen sites, i.e., is a model valid mostly for Cu ions. In addition, it becomes less valid as one moves away from half filling. It is not obvious then that the boundaries for oxygen oscillations follow also approximately the lines of constant J/t_{eff} although with some important deviations, especially at quarter filling. The dependence of K_ρ on J/t and the hole density for the 1D t - J model²⁵ is consistent with the shifting of the Cu $2k_F/4k_F$ boundary to lower values of Δ as hole density $n_h \rightarrow 1$, and in turn this is consistent with the intuitive notion that strongly correlated electrons regimes become more important close to half filling.

However, this mapping does not explain by itself why, in the case of hole doping, the $2k_F/4k_F$ boundaries for O oscillation occur at smaller values of Δ for any given U_p , i.e., why the O subsystem enters the strong correlation regime at smaller interactions than the Cu subsystem. To understand this feature, it would be necessary to analyze effective models obtained by projecting out Cu sites and retaining O sites. These effective models, the so-called “spin-fermion” or

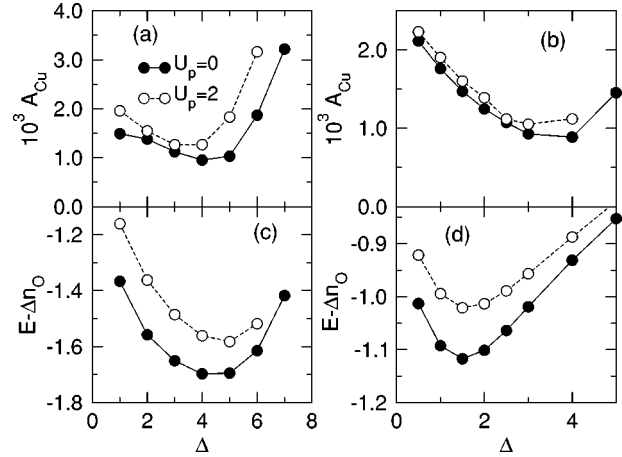


FIG. 7. (a) Average amplitude of Friedel oscillations on Cu sites for $n_h=0.5$. (b) Same for $n_h=0.875$. (c) Corrected ground state energy for $n_h=0.5$. (d) Same for $n_h=0.875$.

Kondo-Heisenberg models,²³ are considerably more complicated and related available results are limited.²⁶ For hole doped cuprates, i.e., with holes in excess of the number of Cu ions, it can be assumed that Cu ions are mostly singly occupied, and in this case our results suggest that the $2k_F$ to $4k_F$ crossover is “driven” by the oxygen oscillations. That is, the O subsystem is more susceptible to strong correlations than the Cu subsystem. On the other hand, for the case of electron doped chains, i.e., with fewer holes than Cu ions, the $2k_F$ to $4k_F$ crossover takes place at small Δ for Cu density oscillations while for O FO’s have $2k_F$ in the range of parameters studied, and in this sense, the crossover seems “driven” by the Cu ions. Hence, the nearly empty O band in electron doped chains is symmetric to the half filled Cu band in hole doped cuprates.

There are two factors affecting the magnitude of the mean amplitudes of the $2k_F$ and $4k_F$ components: their amplitude at the origin, and their power law exponents. The amplitudes at the origin [A_2 , A_3 , B_2 , and B_3 , in Eqs. (A1) and (A2)] may depend on the formation of bound states between holes and impurities. With respect to the power law exponents, one could assume that the FO’s on Cu and on O sites are determined by two different K_ρ since they obey different effective models in addition of having different hole densities. Unfortunately, although the fittings to the oscillations using Eqs. (A1), (A2), and (A3) are very good, the determination of K_ρ from the fitted values is very noisy to allow reliable conclusions. In this sense, an independent study of *periodic* chains, with a careful study of finite size effects, would be necessary to confirm this possibility.

Order of the crossover. It seems to be first order in the sense that there are no other oscillation wave numbers between $2k_F$ and $4k_F$. The evidence of this is rather indirect since our method of fitting does not make room for variable wave numbers, and a Fourier (or windowed Fourier) transform would mix the Friedel oscillations starting from the left and right ends of the open chain. The indication of a first order type of crossover comes from the fact that the overall average amplitude of the density oscillations are minimum at the crossing point [Figs. 1, 4, 7(a) and 7(b)]. This suggests

that the system becomes “frustrated” at the crossing point due to the competition of $2k_F$ and $4k_F$ modulations being unable to develop a modulation at another wave number. The behavior of the corrected ground state energy, $E_0 - \Delta n_O$, [Fig. 7(c) and 7(d)] is consistent with this interpretation: its minimum is located close to the point where A_{Cu} is also at a minimum presumably because it gains energy due to delocalization. Hence, this quantity also suggests that there are no FO with a modulation intermediate between $2k_F$ and $4k_F$.

Predictions. The main prediction of the present study is that CuO chains in $\text{YBa}_2\text{Cu}_3\text{O}_{7-\delta}$ would undergo a $2k_F$ to $4k_F$ crossover in the Friedel oscillations induced by oxygen depletion or by nonmagnetic substitution of Cu ions as doping moves from quarter to half filling and eventually into the electron doped region. Additionally we predict that experiments such as STM, probing O sites, would detect a $4k_F$ modulation while experiments such as neutron scattering would still see a $2k_F$ modulation on Cu sites. More generally, the modulation of FO’s can be considered as a sensible tool to detect the sometimes subtle presence of strong electron correlations in quasi-1D systems. Finally, if the observed modulations in CuO chains are essentially Friedel oscillations and the presence of superconductivity on the planes plays a minor role, then similar modulations should be observed in the non-superconducting compound $\text{PrBa}_2\text{Cu}_3\text{O}_7$ (Refs. 27 and 28).

ACKNOWLEDGMENTS

This work was supported by a Grant-in-Aid for Scientific Research on Priority Areas and the NAREGI Nanoscience Project from MEXT and CREST. One of the authors (M.M.) acknowledges support of 21st Century COE program. The use of supercomputers and friendly technical assistance at the Center for Computational Materials Science, IMR, Tohoku University, is also gratefully acknowledged.

APPENDIX: FITTING PROCEDURE

In general, the oscillation starting from the Cu edge is different to that from the O-edge. The total oscillation, as obtained numerically, is the superposition of both oscillations. Assuming these oscillation follow the Luttinger power law expressions,

$$L(r) \equiv A_0 + A_1 \frac{1}{r} + A_2 \frac{\cos(2k_F r + \phi_1)}{r^{\gamma_1}} + A_3 \frac{\cos(4k_F r + \phi_2)}{r^{\gamma_2}} \quad (\text{A1})$$

and

$$R(r) \equiv B_0 + B_1 \frac{1}{L-r} + B_2 \frac{\cos(2k_F(L-r) + \varphi_1)}{(L-r)^{\eta_1}} + B_3 \frac{\cos(4k_F(L-r) + \varphi_2)}{(L-r)^{\eta_2}}, \quad (\text{A2})$$

where L is the system size, then our fitting function will be

$$S(r) \equiv L(r) + R(r), \quad (\text{A3})$$

with $n_0 < r < L - n_0$. n_0 is the number of sites from each edge that are cut out to avoid wild oscillations. Below, the constant terms A_0 and B_0 are neglected, since a uniform component is subtracted before the fitting process.

The mean amplitudes of the $2k_F$ and $4k_F$ components of the Friedel oscillations starting from the left and from the right edges of the chain are defined as

$$\bar{A}_{2k_F,L} = \frac{A_2}{L-2n_0} \int_{n_0}^{L-n_0} dr \frac{1}{r^{\gamma_1}},$$

$$\bar{A}_{4k_F,L} = \frac{A_3}{L-2n_0} \int_{n_0}^{L-n_0} dr \frac{1}{r^{\gamma_2}} \quad (\text{A4})$$

and

$$\bar{A}_{2k_F,R} = \frac{B_2}{L-2n_0} \int_{n_0}^{L-n_0} dr \frac{1}{r^{\eta_1}},$$

$$\bar{A}_{4k_F,R} = \frac{B_3}{L-2n_0} \int_{n_0}^{L-n_0} dr \frac{1}{r^{\eta_2}}, \quad (\text{A5})$$

respectively.

In the fitting process, Eq. (A3) is rewritten as

$$S(r_i) \equiv A_1 \frac{1}{r_i} + A_2' \frac{\cos(2k_F r_i)}{r_i^{\gamma_1}} + A_2'' \frac{\sin(2k_F r_i)}{r_i^{\gamma_1}} + A_3' \frac{\cos(4k_F r_i)}{r_i^{\gamma_2}} + A_3'' \frac{\sin(4k_F r_i)}{r_i^{\gamma_2}} + B_1 \frac{1}{L-r_i} + B_2' \frac{\cos[2k_F(L-r_i)]}{(L-r_i)^{\eta_1}} + B_2'' \frac{\sin[2k_F(L-r_i)]}{(L-r_i)^{\eta_1}} + B_3' \frac{\cos[4k_F(L-r_i)]}{(L-r_i)^{\eta_2}} + B_3'' \frac{\sin[4k_F(L-r_i)]}{(L-r_i)^{\eta_2}}. \quad (\text{A6})$$

¹D.J. Derro, E.W. Hudson, K.M. Lang, S.H. Pan, J.C. Davis, J.T. Markert, and A.L. de Lozanne, Phys. Rev. Lett. **88**, 097002 (2002).

²M. Maki, T. Nishizaki, K. Shibata, and N. Kobayashi, Phys. Rev. B **65**, 140511 (2002).

³H.A. Mook, P. Dai, K. Salama, D. Lee, F. Dogan, G. Aeppli, A.T. Boothroyd, and M.E. Mostoller, Phys. Rev. Lett. **77**, 370 (1996).

⁴W.E. Pickett, R.E. Cohen, and H. Krakauer, Phys. Rev. B **42**, 8764 (1990).

⁵D.H. Lu, D.L. Feng, N.P. Armitage, K.M. Shen, A. Damascelli, C.

- Kim, F. Ronning, Z.-X. Shen, D.A. Bonn, R. Liang, W.N. Hardy, A.I. Rykov, and S. Tajima, *Phys. Rev. Lett.* **86**, 4370 (2001).
- ⁶H.L. Edwards, A.L. Barr, J.T. Markert, and A.L. de Lozanne, *Phys. Rev. Lett.* **73**, 1154 (1994).
- ⁷Y. Ando, K. Segawa, S. Komiya, and A.N. Lavrov, *Phys. Rev. Lett.* **88**, 137005 (2002).
- ⁸D.N. Basov, R. Liang, D.A. Bonn, W.N. Hardy, B. Dabrowski, M. Quijada, D.B. Tanner, J.P. Rice, D.M. Ginsberg, and T. Timusk, *Phys. Rev. Lett.* **74**, 598 (1995).
- ⁹R. Gagnon, S. Pu, B. Ellman, and L. Taillefer, *Phys. Rev. Lett.* **78**, 1976 (1997).
- ¹⁰B. Grévin, Y. Berthier, and G. Collin, *Phys. Rev. Lett.* **85**, 1310 (2000).
- ¹¹Dirk K. Morr and Alexander V. Balatsky, *Phys. Rev. Lett.* **90**, 067005 (2003).
- ¹²S.R. White, I. Affleck, and D.J. Scalapino, *Phys. Rev. B* **65**, 165122 (2002).
- ¹³A.W. Sandvik and A. Sudbo, *Phys. Rev. B* **54**, 3746 (1996).
- ¹⁴A study of Hubbard chains with alternating on-site energy has been done by K. Penc and F. Mila, *Phys. Rev. B* **50**, 11 429 (1994).
- ¹⁵S. Maekawa and T. Tohyama, *Rep. Prog. Phys.* **64**, 383 (2001).
- ¹⁶S.R. White, *Phys. Rev. Lett.* **69**, 2863 (1992); *Phys. Rev. B* **48**, 10 345 (1993).
- ¹⁷Y. Itoh, T. Machi, C. Kasai, S. Adachi, N. Watanabe, N. Koshizuka, and M. Murakami, *Phys. Rev. B* **67**, 064516 (2003), and references therein.
- ¹⁸H.J. Schulz, *Physica C* **235**, 217 (1994), and references therein.
- ¹⁹See for example, M. Fabrizio and A.O. Gogolin, *Phys. Rev. B* **51**, 17 827 (1995).
- ²⁰G. Bedürftig, B. Brendel, H. Frahm, and R.M. Noack, *Phys. Rev. B* **58**, 10 225 (1998).
- ²¹N. Shibata, K. Ueda, T. Nishino, and C. Ishii, *Phys. Rev. B* **54**, 13 495 (1996).
- ²²A.E. Mattsson, S. Eggert, and H. Johannesson, *Phys. Rev. B* **56**, 15 615 (1997).
- ²³W. Brenig, *Phys. Rep.* **251**, 253 (1995), and references therein.
- ²⁴R.J. Cava, A.W. Hewat, E.A. Hewat, B. Batlogg, M. Marezio, K.M. Rabe, J.J. Krajewski, W.F. Peck, Jr., and L.W. Rupp, Jr., *Physica C* **165**, 419 (1990).
- ²⁵M. Ogata, M.U. Luchini, S. Sorella, and F.F. Assaad, *Phys. Rev. Lett.* **66**, 2388 (1991).
- ²⁶A.E. Sikkema, I. Affleck, and S.R. White, *Phys. Rev. Lett.* **79**, 929 (1997); O. Zachar, *Phys. Rev. B* **63**, 205104 (2001).
- ²⁷T. Mizokawa, C. Kim, Z.-X. Shen, A. Ino, A. Fujimori, M. Goto, H. Eisaki, S. Uchida, M. Tagami, K. Yoshida, A.I. Rykov, Y. Siohara, K. Tomimoto, and S. Tajima, *Phys. Rev. B* **60**, 12 335 (1999).
- ²⁸A.A. Aligia, E.R. Gagliano, and P. Vairus, *Phys. Rev. B* **52**, 13 601 (1995).